Estimation of Hysteretic Damping in Steel Dual Systems with Buckling Restrained Brace and Moment Resisting Frame

Seyed Saeid Tabaee, Omid Bahar

Abstract—Nowadays, energy dissipation devices are commonly used in structures. High rate of energy absorption during earthquakes is the benefit of using such devices, which results in damage reduction of structural elements, specifically columns. The hysteretic damping capacity of energy dissipation devices is the key point that it may adversely make analysis and design process complicated. This effect may be generally represented by Equivalent Viscous Damping (EVD). The equivalent viscous damping might be obtained from the expected hysteretic behavior regarding to the design or maximum considered displacement of a structure. In this paper, the hysteretic damping coefficient of a steel Moment Resisting Frame (MRF), which its performance is enhanced by a Buckling Restrained Brace (BRB) system has been evaluated. Having foresight of damping fraction between BRB and MRF is inevitable for seismic design procedures like Direct Displacement-Based Design (DDBD) method. This paper presents an approach to calculate the damping fraction for such systems by carrying out the dynamic nonlinear time history analysis (NTHA) under harmonic loading, which is tuned to the natural system frequency. Two MRF structures, one equipped with BRB and the other without BRB are simultaneously studied. Extensive analysis shows that proportion of each system damping fraction may be calculated by its shear story portion. In this way, contribution of each BRB in the floors and their general contribution in the structural performance may be clearly recognized, in advance.

Keywords—Buckling restrained brace, Direct displacement based design, Dual systems, Hysteretic damping, Moment resisting frames.

I. Introduction

THE great energy absorption capacity of buckling restrained braces (BRB) is generally accepted. Buckling prevention of steel core in compressional forces and leading that to the yielding point during the earthquake is the concept of using BRB which helps for more stable hysteretic behavior [1]. BRB consists of several components: Restrained yielding steel core, restrained non-yielding segments, unrestrained and non-yielding segment for pin or bolt connection to frame which totally are covered with concrete and encased by a steel tube [2]. Encasing system is effective in both local and overall buckling prevention of the yielding core. Since, it is desirable just for restrained yielding steel core segment to carry the bracing forces in the frame out, providing a sliding film surface between core and encasing system is required. In last

Seyed Saeid Tabaee: M.Sc. Student, Omid Bahar: Assistant Professor are with The International Institute of Earthquake Engineering and Seismology (IIEES), Tehran 1395, Iran (phone: +98-21-22830830; fax: +98-21-22831116; S.Tabaee@iiees.ac.ir, omidbahar@iiees.ac.ir).

year's many experimental tests have been conducted, and results are well suited with the concern finite element analysis. A typical BRB component is shown in Fig. 1 [3].
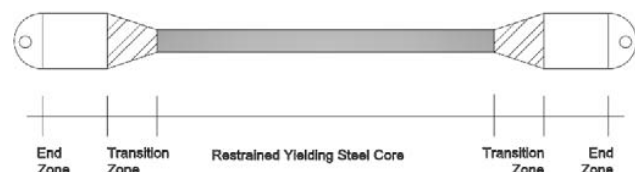

Fig. 1 BRB components

There are different cross section geometries proposed for core of BRB. Fig. 2 shows the common cross sections for BRB [4].
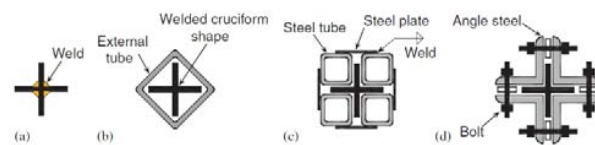

Fig. 2 Common cross-sections for steel BRB

Seismic behavior of frames equipped with BRB is completely different with Non-BRB frames. Indeed hysteresis loops in BRB frames are stable in loading and unloading process during the earthquake; moreover, no degradation in stiffness and strength is appeared, which is expressed in Fig. 3.
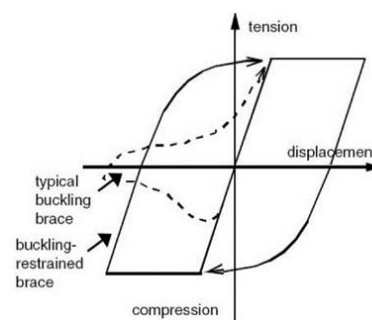

Fig. 3 Force-displacement behavior between BRB and traditional braces

II. Description of the Direct Displacement Based Design (DDBD) Procedure

Performance-based design (PBD) unlike force-base design

(FBD) uses displacement as the input data based on the desired performance level [5]. DDBD is a known PBD procedure which substitutes the structure to equivalent SDOF system. DDBD methodology is presented in Figs. 4 and 5.
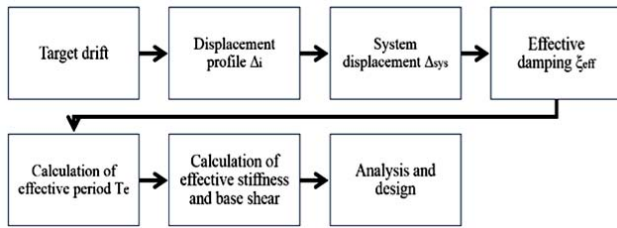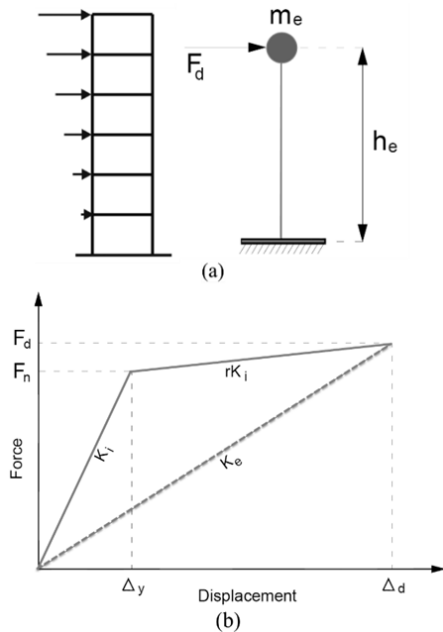

Fig. 4 Design methodology of DDBD

Fig. 5 DDBD for MDOF systems. (a) Equivalent SDOF system, (b) equivalent stiffness and ductility

The design displacement at story i, Δ_i is defined according to the performance level [7]. Displacement profile is calculated regarding to inelastic first mode shape of structure refers to (1):

$$\Delta_i = \delta_i \left(\frac{\Delta c}{\delta_c} \right) \tag{1}$$

where δ_i is the inelastic mode shape and Δc is the design displacement at the critical mass c. δ_c is the value of the mode shape at mass c [6].

m_i is the mass at story i. m_e, the effective mass and Δ_d is equivalent SDOF system design displacement, which refer to (2) and (3), respectively:

$$m_e = \frac{\sum_{i=1}^{n} (m_i \Delta_i)}{\Delta_i} \tag{2}$$

$$\Delta_d = \frac{\sum_{i=1}^{n} (m_i \Delta i^2)}{\sum_{i=1}^{n} (m_i \Delta i)} \tag{3}$$

In order to estimate the equivalent viscous damping (EVD), ductility at the maximum response is used [7]. EVD is a function of different parameters like material, frame system type and hysteretic behavior of structural components, which is the main part of this research, presented in Fig. 6 [6].
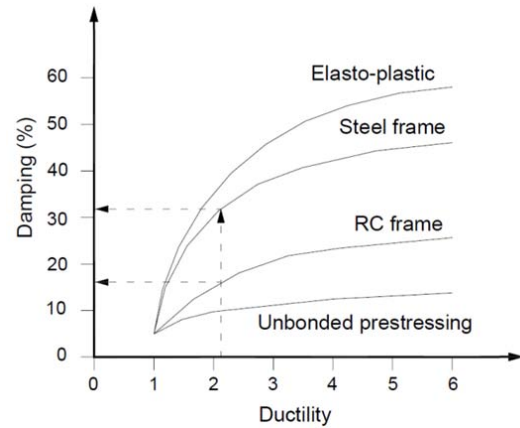

Fig. 6 EVD vs ductility

Effective period, T_e is derived by the Equivalent SDOF system design displacement, Δ_d and calculated EVD. Fig. 7 shows the process [14].
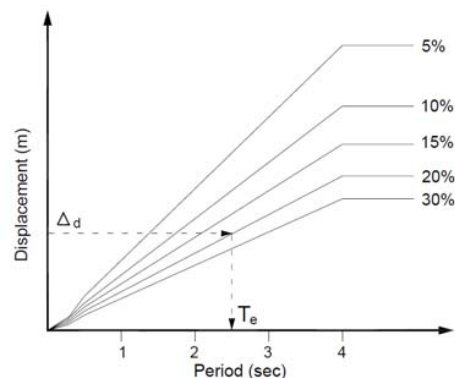

Fig. 7 Design displacement spectra

Effective stiffness and base shear refers to (4) and (5), respectively [6]:

$$K_e = \frac{4\pi^2 m_e}{T_e^2} \tag{4}$$

$$V_{base} = K_e \Delta_e \tag{5}$$

Reviewing the DDBD methodology implies that EVD is a key parameter in the mentioned processes which can affect the analysis results. Thus, in this study there is focused on EVD calculation of an MRF and a dual steel moment frame with BRB.

III. MODELLING

In this study, two structural systems have been evaluated. One of which is an MRF system with moment beam-column connection, and the second system is a combination of an MRF and a BRB system acting as a dual system. The MRF system has been analyzed and designed according to AISC 360-10 [9] and ASCE7-05 [16]. BRB requirements are complied with the manuals, and the story drifts are in allowable ratios [9]. Moreover, since hinge formation at the beam ends has priority to the column hinge formation in PBD, the capacity of beams and columns has been tuned regarding to the nonlinear static analysis.

First, a 3-story, 3-bay MRF has been designed. Each bay is spanned 6 meters, and each floor has 3 meters height. As a second frame, in order to improve seismic behavior and ductility of the designed MRF, three BRB with the same capacity are added in the middle bay of each floor as a diagonal element. This frame is called a dual frame, which is shown in Fig. 8.
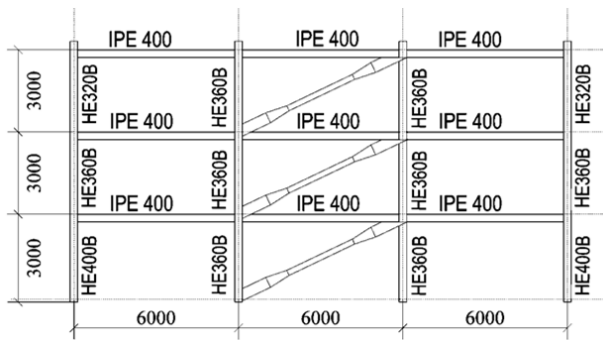

Fig. 8 Dual moment steel frame with BRB

In the PBD procedure, especially in the direct displacement based design method, shortly DDBD, elastic and inelastic mode shapes are desired to conform to each other as much as possible [6]. In this way, the ductility variation over building height will be decreased. This can be achieved by considering beam-sway behavior [7]. In the present dual frame, as mentioned earlier, BRB has uniform strength distribution over the building's height. Nonlinear plastic hinges are assigned to the beams and columns according to the FEMA356 [13]. Force-deformation of BRB has been modelled with a bi-linear link, which is calibrated with experimental tests. When considering compression over-strength regarding to tension strength, compression-strength adjustment factor, β should be evaluated. Strain hardening, ω is another key element beside β. These quantities are defined in (6) and (7) and the bilinear curve is shown in Fig. 9 [10].

$$\beta = \frac{P_{max}}{T_{max}} \qquad (6)$$

$$\omega = \frac{T_{max}}{F_{ysc} A_{sc}} \qquad (7)$$

where A_{sc} is the cross-sectional area of the yielding segment of steel core, F_{ysc} is measured yield strength of the steel core, P_{max} is maximum compression force, and T_{max} is known as maximum tension force within deformations- corresponding to 200% of the design story drift [10].
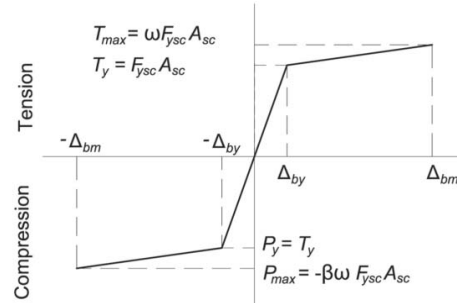

Fig. 9 BRB force-deformation bi-linear

Based on the experimental test results [8], backbone curve according to the normalized maximum deformation was implemented to define BRB behavior as a nonlinear link. Fig. 10 presents the BRB backbone curve. Table I expressed the BRB section details.
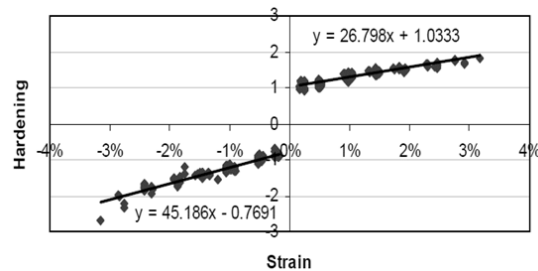

Fig. 10 BRB force-deformation bi-linear link detail

TABLE I
BRB SECTION DETAILS

Story	F_{ysc} (kg/cm^2)	Total Length (cm)	Core Length (cm)	E_{core} kg/cm^2	A_{sc} (cm^2)
3	5554.00	761.00	403.33	2.04E+06	14.19
2	5554.00	761.00	403.33	2.04E+06	14.19
1	5554.00	761.00	403.33	2.04E+06	14.19

When considering MRF, damping is a function of the beams and column hysteretic capacity. In other words, not only plastic hinge's form in beam ends, but also they might be formed in columns. However, in the dual frame, it is possible to let just BRB to yield in earthquakes, while beams and columns are behaving elastic. This can be obtained in BSE-1 earthquake hazard level. Therefore, after the earthquake, BRB can be repaired or replaced. In the present paper, in contrast to BSE-1, maximum capacity of the dual frame is considered, which can be achieved in BSE-2 hazard level. In this case, full damping capacity of the dual system can be obtained by both yielding of BRB and beam, and column hinge's formation.

IV. NONLINEAR TIME HISTORY ANALYSIS (NTHA)

Viscous damping in the dual system can be calculated by nonlinear time history analysis using harmonic loading. Loading frequency is tuned to the first natural frequency of each structure, and the amplitude is chosen to get full hysteretic damping in both dual and MRF frames. Fig. 11 shows the input harmonic loading.
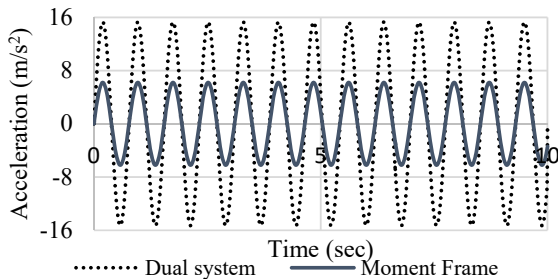

Fig. 11 Harmonic loading

Sweep wave loading (with variable frequency and amplitude) also implemented to find maximum absorbed energy due to hysteretic damping, which is shown in Fig. 12.
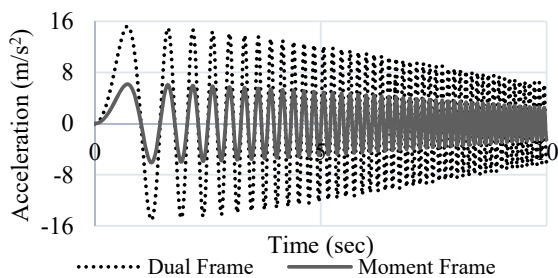

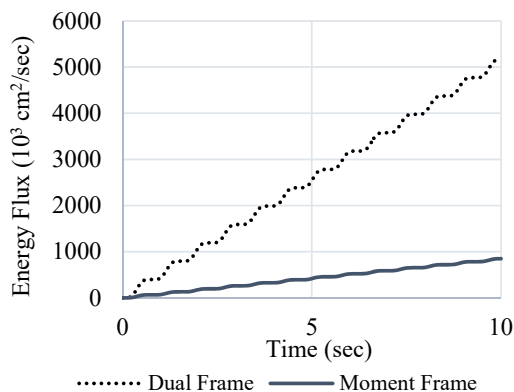Fig. 12 Sweep wave loading

Fig. 13 Energy Flux

When considering the input energy, it is apparent that due to more strength and stiffness capacity of the dual system, it can carry out more input energy than MRF. In order to compare the input energy in both dual and MRF systems, the harmonic and sweep wave loadings were applied with the tuned amplitude to attain the maximum capacity of systems and the plastic hinges formation throughout of the both systems were occurred. Fig. 13 shows the energy flux trend regarding to loading duration.

V. RESULTS

A. Hinges Distribution

NTHA analysis carried out to estimate the damping capacity of both MRF and dual systems. Material (elastic) damping is considered 3 percent in all analyses. Fig. 14 represents the deformation, and plastic hinges formation over the two systems under related harmonic resonance loading.
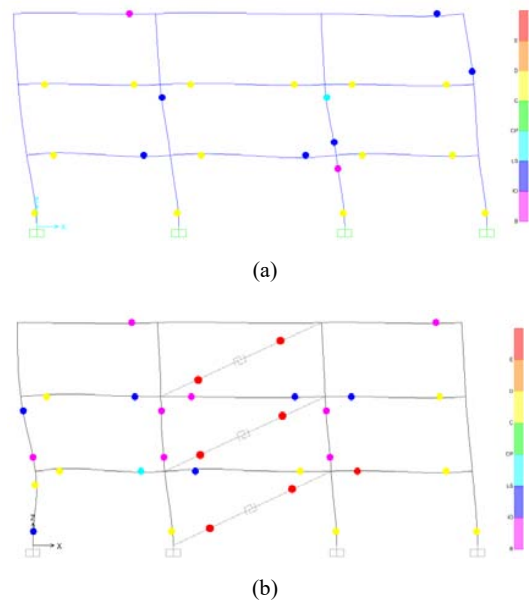

(a)

(b)

Fig. 14 Hinges distribution in maximum capacity. (a) MRF system, (b) Dual system

B. Damping Ratio Calculation

The equivalent system was first presented by Jacobsen [12]. Equivalent damping is a function of the dissipated energy, and it can be calculated in resonance using (8):

$$\xi_{hyst} = \frac{1}{4\pi} \frac{E_D}{E_S} \qquad (8)$$

Where E_D is the damped energy, and E_S is the strain energy [11]. Hysteresis loops of both dual and MRF systems are presented in Fig. 15. Damped energy is calculated based on loop area and strain energy, in the last step of analysis.

Energy absorptions of dual systems are much higher than MRF. This implies from Fig. 14 and the surrounded loop area. Stiffness degradation in MRF is much higher than those of the dual system. Calculated hysteretic damping ratios are tabulated in Table II.

Damping ratios are just related to hysteretic behavior and material damping is not included. The result shows that using BRB not only increases structural stiffness but also improves its hysteretic behavior. In other words, structural ductility is

improved during seismic action. Damping ratio for MRF in its maximum capacity is about 20 percent.
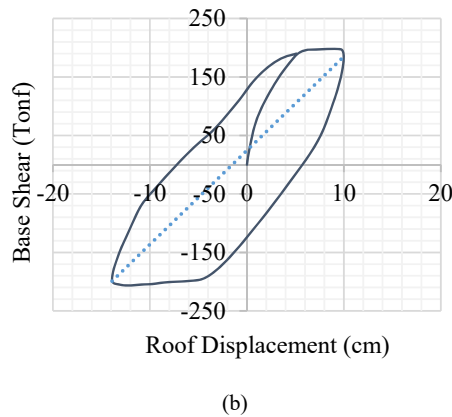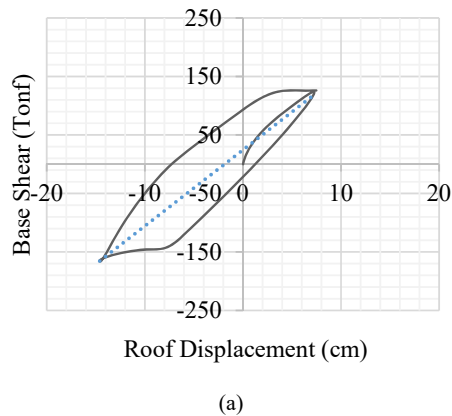

(a)

(b)

Fig. 15 Maximum damping hysteresis loop. (a) MRF system, (b) dual system

TABLE II
DAMPING RATIO AND NATURAL PERIOD

Type	Period (Sec)	Frequency (Cyc/sec)	ξ_{hyst}
Dual Frame	0.322	3.105	0.303
Moment Frame	0.492	2.032	0.204

C. Story Displacement and Shear Values

It can be observed that by adding BRB to the MRF, overall hysteretic capacity is increased. Although in dual systems, the interaction between subsystems is a major point, the effect of BRB in total, damping ratio is reasonably apparent. Maximum and minimum story displacement in both MRF and BRB is presented in Fig. 16.

It is obvious that, the dual system with higher stiffness and greater damping capacity has lower displacement rates, compared to MRF. In the considered dual system, BRB implementation in MRF also affects story shears. In Fig. 17 distributions of story shears along the height of the dual and MRF systems are shown.

Story shear is variable during loading time steps; meanwhile, at the maximum hysteretic behavior time steps, the story shears are presented. Although the input energy of

dual system is clearly much more than MRF system, lower displacement values are resulted in the dual systems this can be inferred by comparing Figs. 16 and 17.
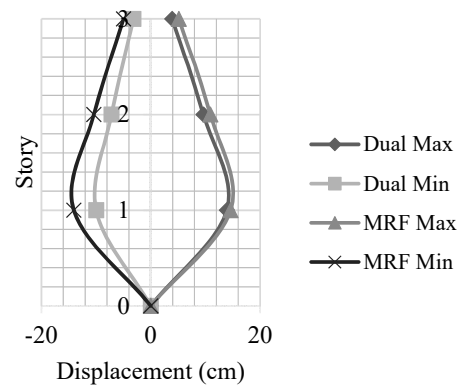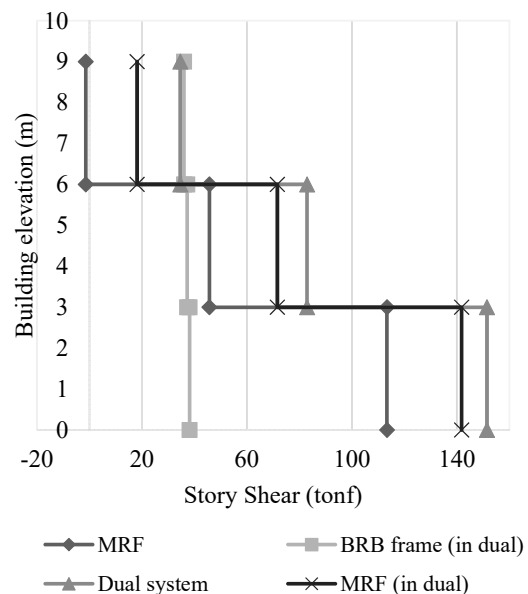

Fig. 16 Maximum and minimum story displacement

Fig. 17 Story shear distribution over height

Dual System Damping Ratios Comparison

Dual system has a capacity to carry more shear forces in comparison with MRF frame. The greater floor shear forces part are related to the capacity of the MRF in the dual system. This is confirmed by plastic hinge's formation in beams and columns of MRF in the dual frame with respect to the bare MRF frame. It is noted that, MRF is the same in both cases.

In this research BRB has uniform strength distribution over the building's height; however, if the MRF strength distribution over the building's height is uniform, DDBD concepts of displacement profile should be considered.

A single BRB is loaded harmonically to achieve its maximum damping ratio. This is carried out based on the bilinear force-deformation experimental information which is
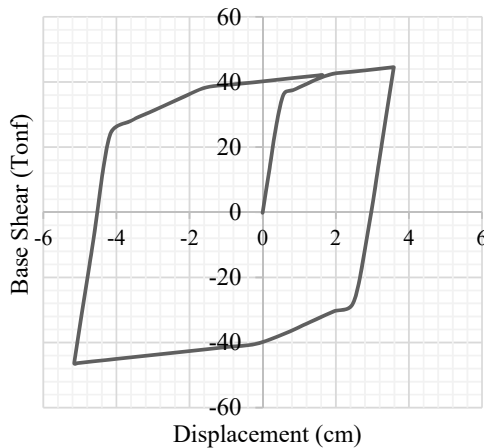
presented in Fig. 18.

Fig. 18 Single BRB hysteresis curve

Maximum damping ratio of BRB, ζ_{hyst} (from NTHA) is determined as 47.4 percent. In analysis, story shear proportion and distribution between each subsystem of the dual system is investigated. Furthermore, each subsystem maximum damping ratio as calculated in earlier steps are considered. It has been found that without any prior information about the dual system hysteretic capacity, just based on the maximum story shear, a proportion of each subsystems and their related maximum damping ratios, the total damping ratios of dual system referring to (9) can be derived, and its results are presented in Tables III and IV [15].

$$\zeta_{dual} = \frac{\zeta_{moment} V_{moment} + \zeta_{brb} V_{brb}}{V_{moment} + V_{brb}} \qquad (9)$$

ζ_{moment} is the maximum damping capacity of subsystem moment frame in the dual system and ζ_{brb} is the maximum damping capacity of brb frame included in the dual system. The shear values are calculated in dual system due to each subsystem shear portion.

TABLE III
STORY SHEAR DISTRIBUTION AT MAXIMUM TIME STEP

Story	BRB Shear (Tonf)	MRF (Tonf)
3	36.008	-1.434
2	37.213	45.677
1	38.114	113.339

TABLE IV
DAMPING ESTIMATION ACCORDING TO STORY SHEAR

ζ_{moment}	ζ_{brb}	ζ_{dual}	ζ_{hyst}
0.204	0.474	0.316	0.303

According to Table IV, ζ_{dual} calculated referred to (9), is nearly equal to ζ_{hyst} which is based on NTHA analysis under cyclic loading, which was calculated in Table II. Although there is a little difference between mentioned damping ratios, this can be justified as subsystem interaction.

In DDBD procedure calculation of the effective period, T_e is directly depended on the reduced design response spectrum of displacement based on damping ratio. Indeed for dual systems ζ_{hyst} can be investigated in advance using (9), which is a merit in performance-based design, specifically DDBD procedure.

VI. CONCLUSION

In conclusion, this research has been suggested a way to determine damping ratio of the dual system just by estimating subsystems maximum damping ratios and their story shear portion in the dual system. This is useful in DDBD procedure when choosing displacement response spectra. In future, more analyses might be performed to consider the number of story effects, specifically when higher modes, affect the analysis results.

REFERENCES

[1] Kim J, Seo Y. Seismic design of low-rise steel frames with buckling-restrained braces. Engineering Structures 2004; 26(5):543–51.
[2] Kim J, Choi H. Behavior and design of structures with buckling-restrained braces. Engineering Structures 2004; 26(6):693–706
[3] Sahoo DR, Chao SH. Performance-based plastic design for buckling-restrained braced frames. In: Proceedings of 9th US national and 10th Canadian conference on earthquake engineering. 2010 (in press).
[4] Zhao, J., Wu, B. and Ou, J. (2011), a novel type of angle steel buckling-restrained brace: Cyclic behavior and failure mechanism. Earthquake Engng. Struct. Dyn, 40: 1083–1102.
[5] Aidcer L. Vidot-Vega, Mervyn J. Kowalsky, Drift, strain limits and ductility demands for RC moment frames designed with displacement-based and force-based design methods, Engineering Structures, Volume 51, June 2013, Pages 128-140
[6] Priestley MJN, Calvi GM, Kowalsky MJ. Displacement-based seismic design of structures. IUSS Press; 2007 (721pp.).
[7] Maley TJ, Sullivan TJ, Della Corte G. Development of a displacement-based design method for steel dual systems with buckling-restrained braces and moment-resisting frames. Journal of Earthquake Engineering 2010; 14(S1): 106–40.
[8] Romero P, Reaveley L, Miller P, Okahashi T (2003) Full-scale testing of WC Series buckling-restrained braces, Department of Civil and Environmental Engineering, University of Utah, USA
[9] ANSI/AISC 360-10, Specification for Structural Steel Buildings, American Institute of Steel Construction, USA 2010.
[10] AISC. ANSI/AISC 341-10. Seismic provisions for structural steel buildings. Chicago (IL): American Institute of Steel Construction; 2010.
[11] Chopra AK, Goel RK. Building period formulas for estimating seismic displacements. Earthquake Spectra 2000; 16(2):533–6.
[12] Jacobsen, L. S. (1930) "Steady forced vibrations as influenced by damping," ASME Transactione 52(1), 169–181.
[13] Federal Emergency Management Agency. Prestandard and commentary for the seismic rehabilitation of buildings. Report FEMA 356, Washington, DC, 2000.
[14] Garcia, R., Sullivan, T. J., and Della Corte, G. (2009) ''Development of a displacement-based design method for steel frame-RC wall buildings'' Journal of Earthquake Engineering 14(2), 252–277.
[15] Fabio Mazza, Alfonso Vulcano, 2014. Design of Hysteretic Damped Braces to Improve the Seismic. Ingegneria Sismica. , pp.5-16
[16] ASCE 7-05. Minimum design load for buildings and other structures. Reston (VA): American Society of Civil Engineers; 2005.